Supporting Information

In_2S_3/HOF S-scheme heterojunction for enhanced photocatalytic H_2O_2 production

Yong Zhang[a], Wenjun Zhu[a,*], Yanyan Zhao[b], Shumin Zhang[c]

[a]*School of Advanced Materials and Green Chemical Engineering, Hubei Provincial Engineering Research Center for Chemical Additives of Polymeric Materials, Hubei polytechnic University, Huangshi 435003, Hubei, China*

[b]*College of Biology Pharmacy and Food Engineering, Shangluo University, Shangluo 726000, Shaanxi, China*

[c]*Hunan Key Laboratory of Applied Environmental Photocatalysis, Changsha University, Changsha 410022, Hunan, China*

1. Chemicals and materials

All chemicals and solvents were commercially available products and used without further puriffcation. Methanol, ethanol, benzyl alcohol, acetone, glycerol, N,N-dimethyl formamide (DMF), thioacetamide (TAA) and $InCl_3$ were purchased from Bidepharm (China). 1,3,6,8-tetra(4-carboxylphenyl) pyrene (H_4TBAPy) was bought from Jilin Chinese Academy of Sciences-Yanshen Technology Co., Ltd.

2. Characterization

X-ray power diffraction (XRD) patterns were performed on a X-ray diffractometer (Shimadzu XRD-6100, Japan). Thermogravimetric analysis (TGA) was examined using a thermal analyzer (Shimadzu DTG-60H, Japan). Fourier transform infrared (FTIR) spectra were recorded on a spectrometer (Nicolet iS50, Thermo Scientific, USA). UV–visible diffuse reflection spectra were obtained on a UV–vis spectrophotometer (Shimadzu UV2600, Japan). Transmission electron microscopy (TEM) images and high-resolution transmission electron microscopy (HRTEM) images were conducted on a microscope (JEM-F200, Japan). Field-emission scanning electron microscopy (FESEM, JSM 7500F, Japan) was used to observe the morphology of samples. X-ray photoelectron spectroscopy (XPS) were carried out on an ESCALAB 250 spectrometer with monochromatic Al Kα (1486.6 eV) X-ray source (Thermo Fisher Scientific, USA), and the binding energies were calibrated by the C 1s peak at 284.6 eV from the adventitious carbon. The Brunauer-Emmett-Teller (BET) specific surface area (S_{BET}) of the samples was determined by nitrogen adsorption in a nitrogen adsorption apparatus (TriStar II 3020, USA). Photoluminescence (PL) spectra of the samples were analyzed by a fluorescence spectrophotometer (FLS 1000, Edinburgh, UK). Time-resolved photoluminescence (TRPL) spectra were analyzed by a fluorescence lifetime spectrophotometer (FLS 1000, Edinburgh, UK). Electron paramagnetic resonance (EPR) spectra were obtained on an EPR spectrometer (MEX-nano, Bruker, Germany) by using 5,5-dimethyl-1-pyrrolidine N-oxide (DMPO) as the spin trapping agent. Femtosecond transient absorption spectroscopy (fs-TAS) was measured on a pump-probe system (Helios Fire, Ultrafast System) with a maximum time delay of ~8 ns, controlled by a motorized optical delay line.

3. Photocatalytic H_2O_2 production

Photogenerated H_2O_2 tests were performed in an open offline photocatalytic reactor (MC-GF80, Merry Change, China), and the reaction temperature was kept constant at 20 °C with circulating water pump. The reactor was irradiated with a 300 W xenon lamp equipped with a cutoff filter (λ > 420 nm). Typically, 10 mg of as-prepared sample was ultrasonically dispersed in 1% benzyl alcohol aqueous solution (50 mL), and the resultant dispersion was stirred in air for 30 min. Afterward, the the photocatalytic reaction was triggered by using a 300 W xenon lamp. During the measurements, 0.5 mL of aliquot was extracted from the reaction system every 15 min. To remove the insoluble photocatalyst, it's filtered through a 0.45 μm microporous membrane. The H_2O_2 concentration was determined using iodometry method [1]. Cycling experiments were performed for 4 repeated times by the same method mentioned above. Used sample was obtained by centrifugation in each cycle, and then rinsed with water before reuse. The degradation tests were conducted in nitrogen atmosphere using 1 mmol L^{-1} H_2O_2 [2].

4. Kinetics analysis of H_2O_2

Kinetic analysis is performed to evaluate the formation and decomposition rate constants of H_2O_2 during photocatalysis. The kinetic constants are calculated by fitting the H_2O_2 production curves via the equation (1) and (2), where t stands for the irradiation time, and K_f [μmol L^{-1} min^{-1}] and K_d [min^{-1}] are the rate constants for H_2O_2 formation and decomposition, respectively.

$$[H_2O_2] = K_f / K_d \times [1 - \exp(-K_d t)] \quad \text{(S1)}$$

$$\ln(C_0/C) = K_d t \quad \text{(S2)}$$

5. Apparent quantum yield (AQY) calculation

Incident light of different wavelengths (λ = 420 nm, 450 nm, 500 nm and 600 nm) was chosen as the light source to trigger the photocatalytic reaction, and the apparent quantum efficiency (AQE) was calculated after 1 h irradiation. The average irradiation intensity is determined to be 3.8 mW cm^{-2} and the irradiation area is 12 cm^2. Take 420 nm incident light

for example, the number of incident photons (N) is 3.37 × 10^{20} as calculated by equation (S3).

$$N = \frac{E\lambda}{hc} = \frac{3.8\times10^{-3}\times12\times3600\times420\times10^{-9}}{6.626\times10^{-34}\times3\times10^{8}} = 3.37\times10^{20} \quad \text{(S3)}$$

The amount of H_2O_2 molecules generated in 1 h is 17.5 μmol. The AQY is calculated from the following equation (S4).

$$\text{AQY} = \frac{2\times \text{the number of evolved } H_2O_2}{\text{the number of incident photons}} \times 100 \quad \text{(S4)}$$

$$= \frac{2\times6.02\times10^{23}\times17.5\times10^{-6}}{3.37\times10^{20}}$$

$$= 6.25\%$$

6. Rotating disk electrode (RDE) measurements

The rotating disk electrode was used as the substrate for the working electrode. 10 mg of the catalyst was dispersed in a mixture consisting of 0.5 mL of ethanol and 20 μL of Nafion solution (5 wt%). The resulting mixture was sonicated to create a uniform catalyst ink. Then, 20 μL of the slurry was applied onto the disk electrode, which was subsequently allowed to dry at room temperature. The rotating disk electrode served as the substrate for the working electrode. Carbon rods and Ag/AgCl electrodes were used as counter and reference electrodes, respectively. Linear sweep voltammetry (LSV) was obtained at room temperature in O_2-saturated 0.1 M phosphate-buffered saline (PBS, pH = 7) solutions at with a scanning rate of 10 mV s^{-1}. The average number of electrons (n) was calculated by Koutecky-Levich equation:

$$J^{-1} = J_K^{-1} + B^{-1}\omega^{-1/2} \quad \text{(S5)}$$

$$B = 0.62nF\upsilon^{-1/6}C_0D_0^{2/3} \quad \text{(S6)}$$

where J is the current density, J_K is the kinetic current densities, ω is the rotating speed (rpm), n is transferred electron number, F is Faraday constant (96485 C mol^{-1}), C_0 is the volume concentration of O_2 (1.26 ×10^{-3} mol cm^{-3}), D_0 is the diffusion coefficient of O_2 (2.7 ×10^{-5} cm^2 s^{-1}), and ν is kinetic viscosity of the electrolyte (0.01 cm^2 s^{-1}).

7. Computational details

Density functional theory (DFT) calculations were carried out by using the Vienna Ab

initio Simulation Package (VASP). The exchange–correlation interaction was described by generalized gradient approximation (GGA) with the PBE functional. The energy cutoff was set to 450 eV. The convergence threshold in geometry optimization was set to 10^{-5} eV for energy and 0.03 eV/Å for force. For the construction of PFC-1 and In_2S_3 (110) surface models, a vacuum slab of 15 Å and 20 Å was used to eliminate interactions between periodic structures, respectively.

8. Supplementary figures and tables

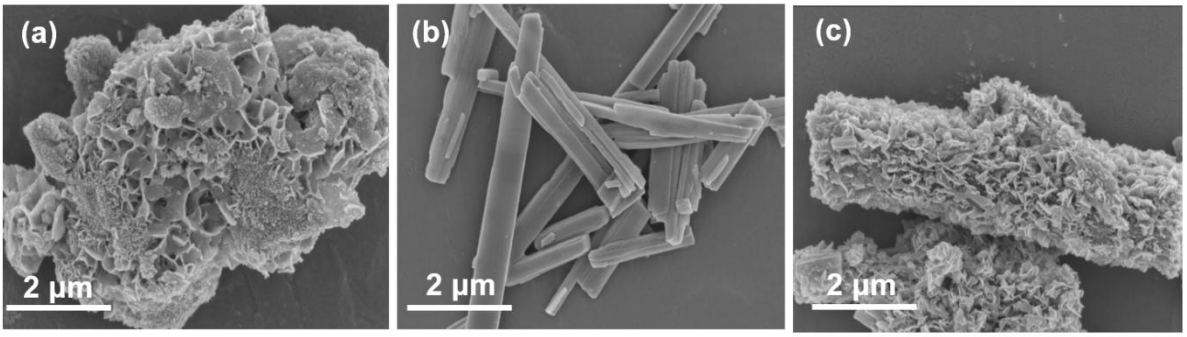

Fig. S1 SEM images of (a) In_2S_3, (b) PFC-1, and (c) IP-40.

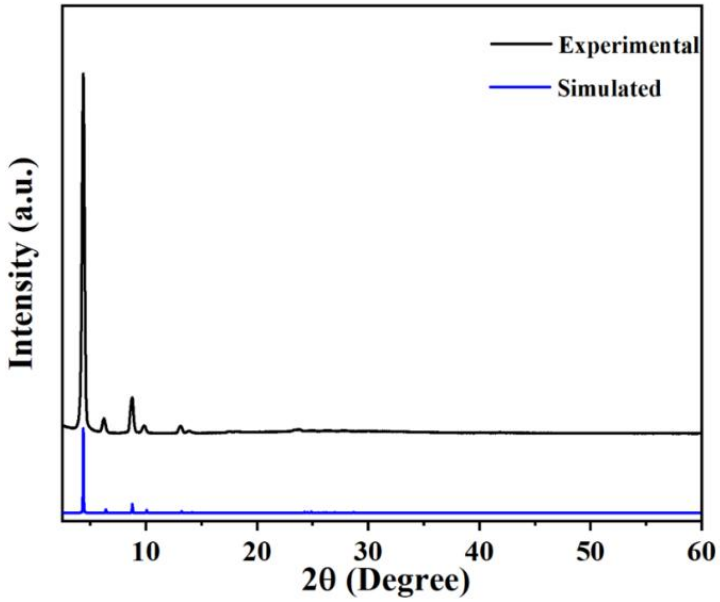

Fig. S2 The experimental and simulated PXRD patterns of PFC-1.

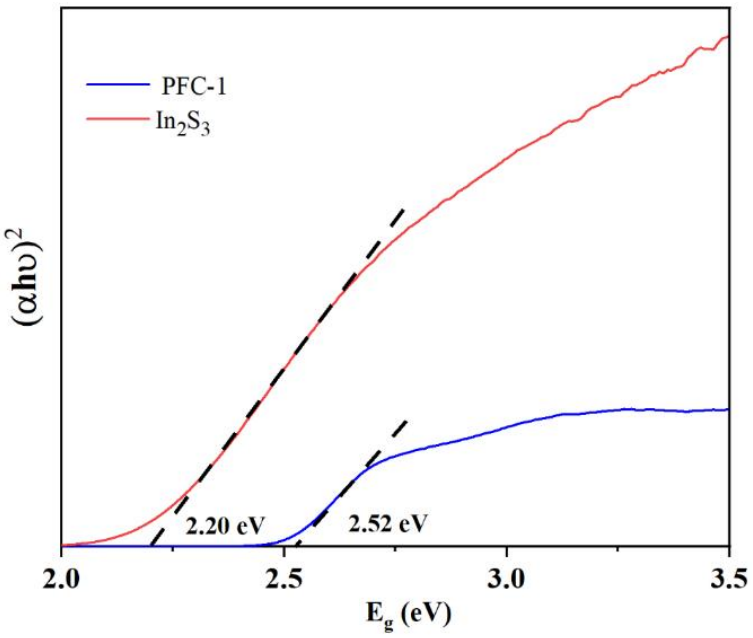

Fig. S3 Tauc plots of In_2S_3 and PFC-1.

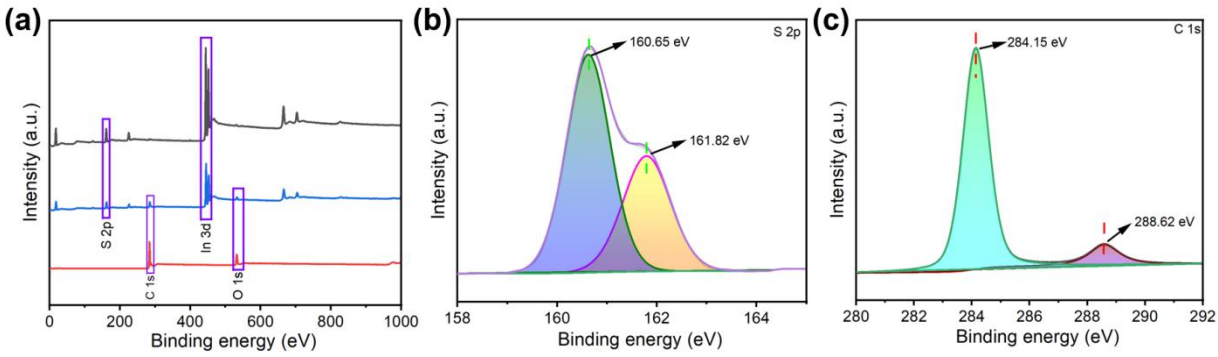

Fig. S4 (a) XPS survey spectra of In_2S_3, PFC-1 and IP-40. XPS spectra of (b) S 2p and (c) C 1s of IP-40.

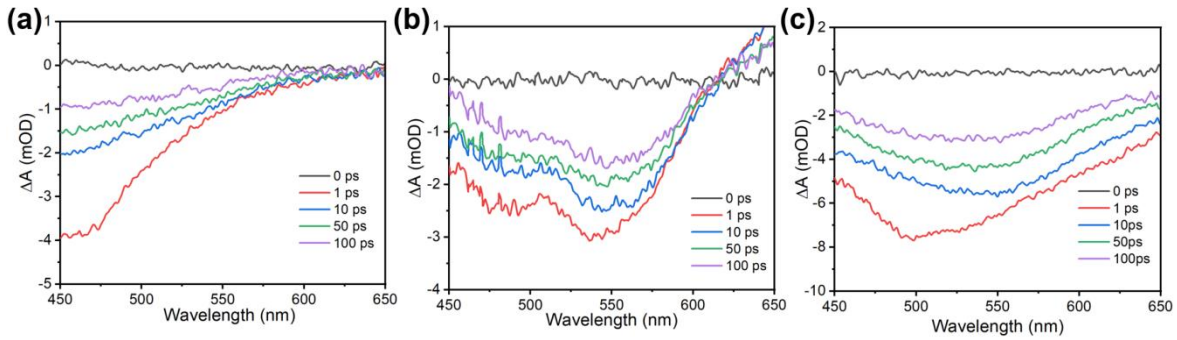

Fig. S5 Fs-TAS spectra recorded at the indicated delay times for (a) In_2S_3, (b) PFC-1, and (c) IP-40.

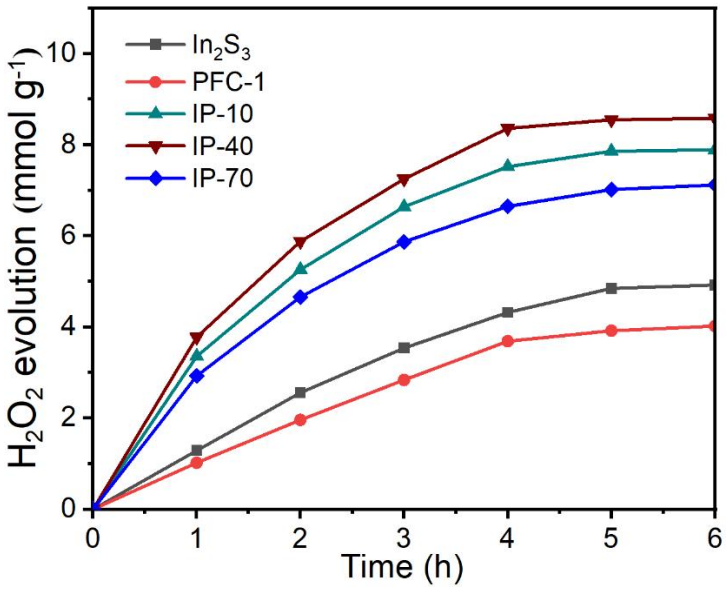

Fig. S6. The influence of time on photocatalytic H_2O_2 production over as-prepared samples.

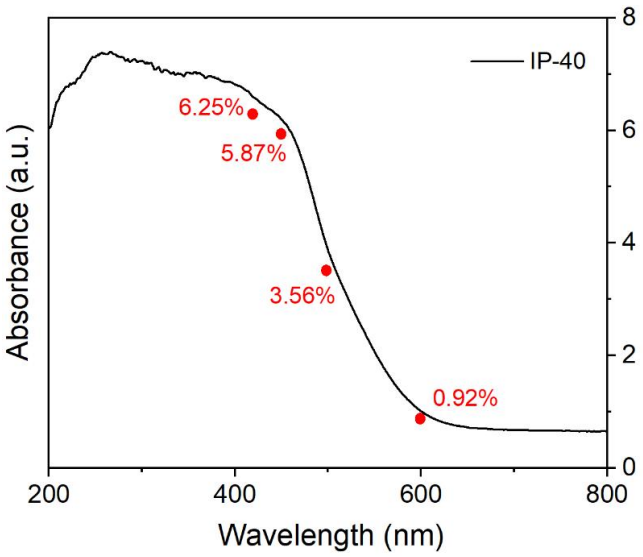

Fig. S7 AQE obtained at different incident light wavelengths (420, 450, 500 and 600 nm) versus absorption spectrum of IP-40.

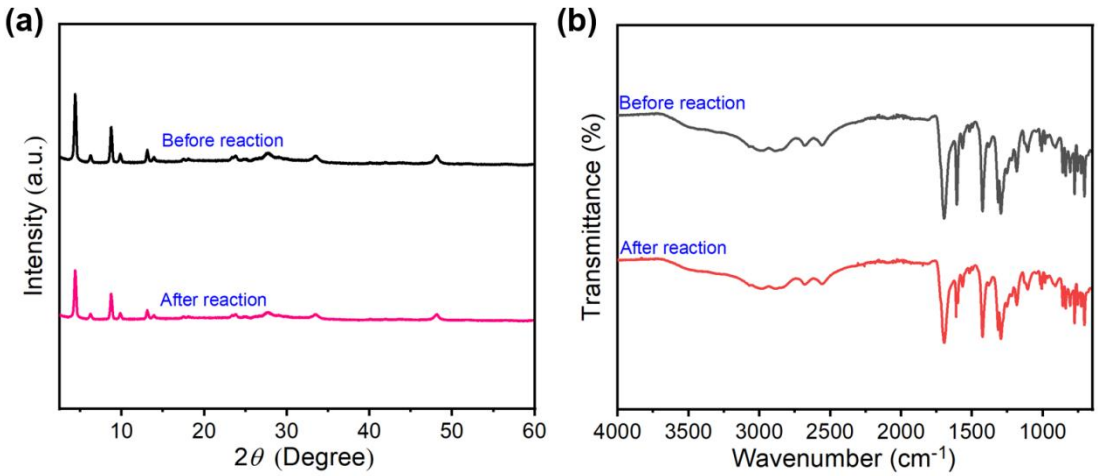

Fig. S8 (a) PXRD patterns and (b) FTIR spectra of IP-40 sample before and after photocatalytic H_2O_2 production.

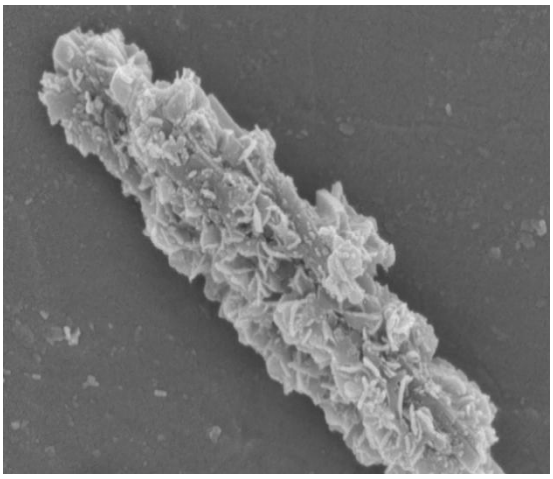

Fig. S9 FESEM image of IP-40 after photocatalytic reaction.

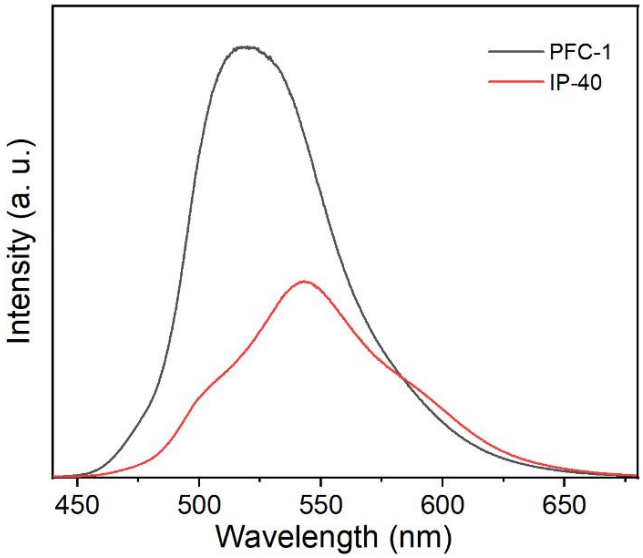

Fig. S10 Photoluminescence spectra of IP-40 and PFC-1.

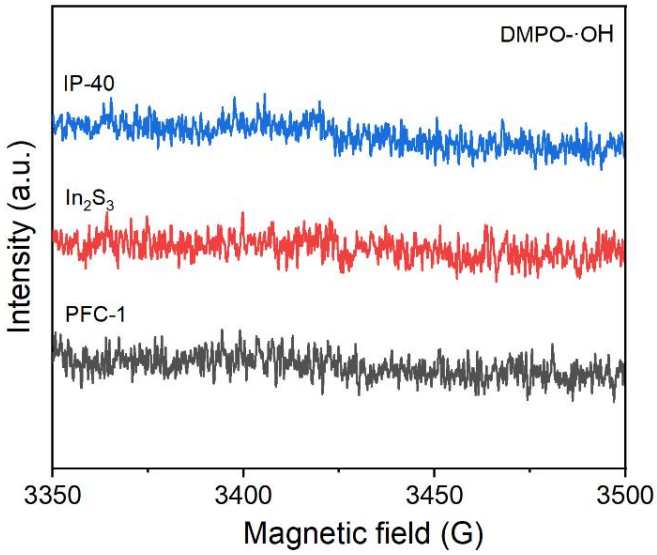

Fig. S11 EPR signals of DMPO-·OH of PFC-1, In_2S_3 and IP-40 in water after 5 min irradiation.

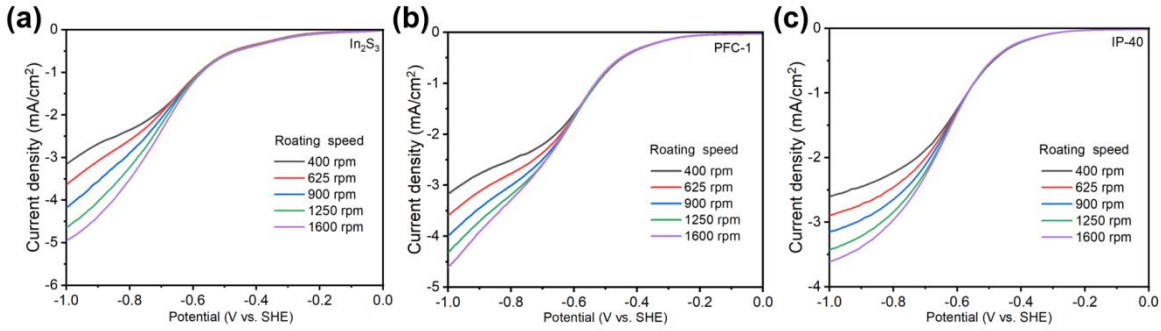

Fig. S12 LSVcurves of (a) In_2S_3, (b) PFC-1, and (c) IP-40 on the rotating disk electrode at different rotation speeds.

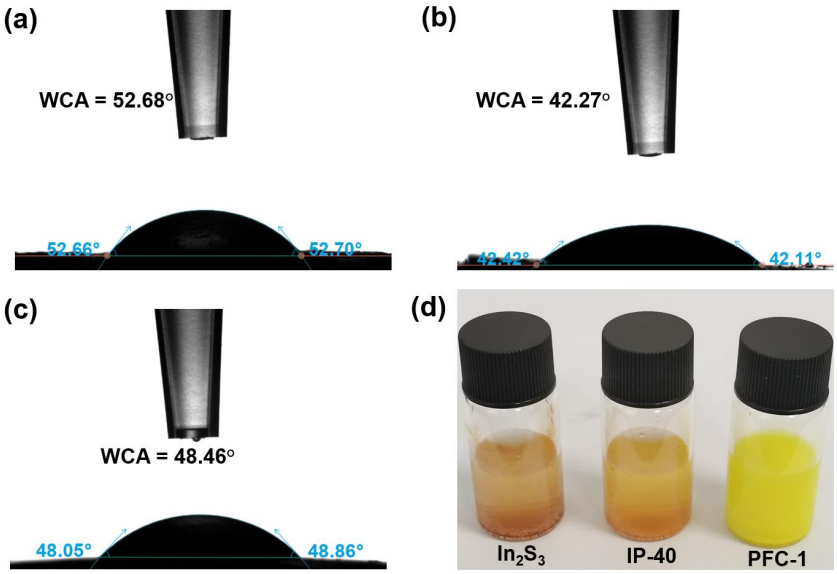

Fig. S13 The water contact angle patterns of (a) PFC-1, (b) In_2S_3 and (c) IP-40. (d) The image of ultrasonic dispersion of the prepared samples in water.

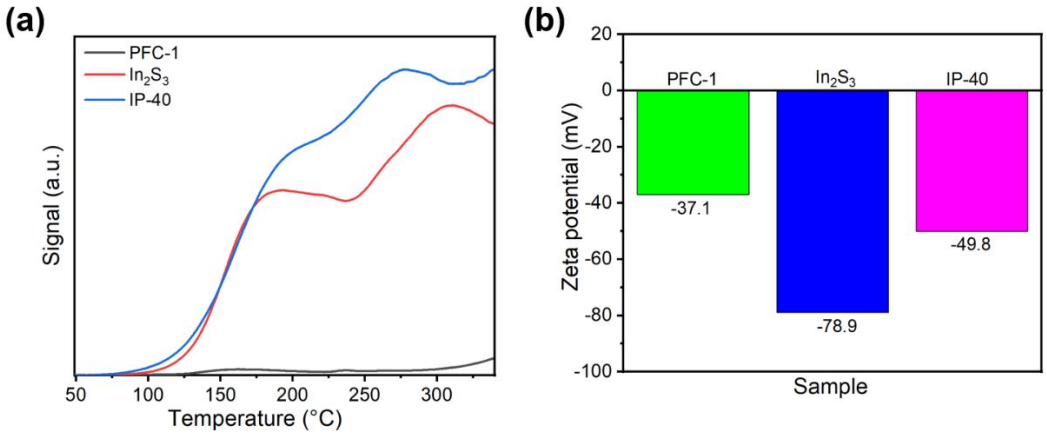

Fig. S14 (a) Oxygen temperature-programmed desorption (O_2-TPD) curves, (b) zeta potentials of the samples.

Table S1 Surface area, pore size and pore volume of In_2S_3, PFC-1 and IP-40.

Sample	S_{BET} (m^2/g)	V_{pore} (cm^3/g)	d_{pore} (nm)
In_2S_3	72	0.21	11
PFC-1	1351	0.84	2.5
IP-40	458	0.81	7.1

Table S2 Fitting parameters for the fs-TAS decay kinetics of In_2S_3 and IP-40 at 460nm.

Sample	τ_1 (ps)	A_1 (%)	τ_2 (ps)	A_2 (%)	τ_3 (ps)	A_3 (%)	T_{ave} (ps)
In_2S_3	3.08	50.73	72.07	49.27			69.16
IP-40	2.56	0.5571	85.44	0.4429			82.43

Table S3 Fitting parameters for the fs-TAS decay kinetics of PFC-1 and IP-40 at 540nm.

Sample	τ_1 (ps)	A_1 (%)	τ_2 (ps)	A_2 (%)	τ_3 (ps)	A_3 (%)	τ_{ave} (ps)
PFC-1	2.31	51.98	83.11	48.02			80.75
IP-40	1.03	2.76	105.72	31.97	12.81	65.27	87.24

Table S4 Photocatalytic H_2O_2 production performance of different organic framework-based photocatalysts in the previously reported literatures.

Photocatalysts	Energy source	Scavenger	H_2O_2 yield (mmol g^{-1} h^{-1})	Ref.
$ZnIn_2S_4$/UiO-66-NH_2	300 W Xe lamp (λ= 400−780 nm)	H_2O	0.80	[3]
UiO-66-B	Solar simulator (λ≥360 nm)	isopropanol	1.00	[4]
ZnSe/COF	300 W Xe lamp (λ≥420 nm)	ethanol	1.89	[5]
TiO_2/COF	300W Xe lamp (λ= 350−780 nm)	furfuryl alcohol	1.48	[6]
ZnO/COF	Solar simulator (λ≥360 nm)	ethanol	2.44	[7]
BiOBr/COF	300W Xe lamp (λ≥360 nm)	ethanol	3.75	[8]
$MgIn_2S_4$/COF	300W Xe lamp (λ≥420 nm)	H_2O	4.25	[9]
In_2S_3/COF	300 W Xe lamp (λ≥420 nm)	H_2O	0.69	[10]
TTF-Bpy-HOF	300 W Xe lamp (λ≥420 nm)	H_2O	0.68	[11]
PTBA	300 W Xe lamp (λ≥420 nm)	benzyl alcohol	2.69	[12]
In_2S_3/PFC-1	300 W Xe lamp (λ≥420 nm)	benzyl alcohol	3.78	This work

Table S5 Fitting parameters for the TPRL decay curves of In_2S_3, PFC-1, and IP-40.

Sample	τ_1 (ns)	A_1 (%)	τ_2 (ns)	A_2 (%)	τ_3 (ns)	A_3 (%)	τ_{Ave} (ns)
In_2S_3	0.48	11.51	1.92	59.93	6.97	28.55	3.20
PFC-1	0.50	8.75	2.13	70.45	5.63	20.80	2.72
IP-40	0.71	13.16	2.24	81.70	8.90	5.13	2.38

References

[1] J. Qiu, K. Meng, Y. Zhang, B. Cheng, J. Zhang, L. Wang, J. Yu, Adv. Mater., **2024**, 36, 2400288.

[2] Y. Zhang, J. Qiu, B. Zhu, G. Sun, B. Cheng, L. Wang, Chin. J. Catal., **2024**, 57, 143-153.

[3] J. Qiu, L. Zhang, G. Xia, D. Dai, Y. Tang, J. Yao, Catal. Sci. Technol., **2023**, 13, 2101-2107.

[4] Y. Li, F. Ma, L. Zheng, Y. Liu, Z. Wang, P. Wang, Z. Zheng, H. Cheng, Y. Dai, B. Huang, Mater. Horiz., **2021**, 8, 2842-2850.

[5] Y. Zhao, C. Yang, S. Zhang, G. Sun, B. Zhu, L. Wang, J. Zhang, Chin. J. Catal., **2024**, 63, 258-269.

[6] Y. Yang, J. Liu, M. Gu, B. Cheng, L. Wang, J. Yu, Appl. Catal. B: Environ., **2023**, 333, 122780.

[7] Y. Zhang, J. Qiu, B. Zhu, M. Fedin, B. Cheng, J. Yu, L. Zhang, Chem. Eng. J., **2022**, 444, 136584.

[8] H. Zhang, J. Liu, Y. Zhang, B. Cheng, B. Zhu, L. Wang, J. Mater. Sci. Technol., **2023**, 166, 241–249.

[9] Y. Zhang, Y. Wang, Y. Liu, S. Zhang, Y. Zhao, J. Zhang, J. Materiomics, **2025**, 11, 100985.

[10] H. Chen, S. Gao, G. Huang, Q. Chen, Y. Gao, J. Bi, Appl. Catal. B: Environ., **2024**, 343, 123545.

[11] J. Zhang, Z. Ge, J. Wang, D. Zhong, T. Lu, Nat. Commun., **2025**, 16, 2448.

[12] M. Hu, C. Wu, S. Feng, J. Hua, Molecules, **2023**, 28, 6850.